*36th EPS Conference on Plasma Phys. Sofia, June 29 - July 3, 2009 ECA Vol.**33E**, O-5.056 (2009)*

Flushing and Erosion of Tungsten during Edge Localised Modes

R. Dux, T. Pütterich, A. Janzer, and the ASDEX Upgrade Team

Max-Planck-Institut für Plasmaphysik, EURATOM Association, Garching, Germany

Introduction

In ASDEX Upgrade, the transition from carbon based plasma facing components towards a full tungsten machine offers the opportunity to study the erosion and transport of a high-Z element. In H-mode discharges with type-I ELMs, the tungsten production at the plasma facing components is dominated by the erosion during ELMs. Nevertheless, discharges with lower ELM frequency have higher tungsten concentration in the confined plasma and a minimum ELM frequency of about 80 Hz is required to perform long steady discharges with constant tungsten concentration. The ELM frequency is usually increased by increasing the deuterium puff level. The flushing of tungsten from the confined plasma during the ELM seems to be the dominant effect compared to the expected increase of tungsten production. In order to disentangle the effects of production and flushing of tungsten during an ELM cycle, the experimental situation of a series of discharges #22895-#22901 with varying ELM frequency was modelled with the impurity transport code STRAHL. The experimental results were presented in [1].

The Impurity Transport Model

The STRAHL code [2] solves the radial continuity equation for each ionised stage of an impurity. For the radial transport turbulent diffusion coefficients and drift velocities are set ad hoc, while a full treatment of the neo-classical transport parameters is included. The background plasma parameters like n_e, T_e and T_i are taken from the experiment. The calculation domain extends into the scrape-off layer. Here, the parallel transport towards the divertor or to the limiting elements in the main chamber is described by volumetric losses with a loss frequency, that is given by the parallel connection length between the surface elements $L_{||}$ and the mean flow velocity of the deuterium ions: $v_{||} = (2M//L_{||})\sqrt{k_B(3T_i+T_e)/m_D}$, where the Mach number M was set to 0.1 for the presented results. At a certain radius in the SOL, the main chamber limiters are introduced into the code by switching the connection length from 50 m to 1 m. The neutral impurities start with a prescribed rate at this limiter position. They have a constant radial velocity v_0 and their density decays radially according to the rate $\nu_{ion} = n_e\langle\sigma_{ion}\mathrm{v_e}\rangle$ for ionisation: $n_0(r) = n_0(r_{lim})(r_{lim}/r)\exp[-\int(\nu_{ion}/\mathrm{v}_0)\mathrm{d}r]$.

For this work, the code was enhanced to model light impurities and tungsten during one run in order get a more realistic description of the tungsten behaviour during the ELM cycle. For the shown results carbon and oxygen were included. The tungsten erosion is mainly due to physical sputtering by light impurities and the new version allows to calculate the influx rate of neutral tungsten from the loss of light impurity ions onto the limiter and the sputtering yield [3]. Here, the yield for normal incidence is used, which is a function of impurity mass and energy. The energy at the surface is approximated by $E = k_B(2T_i + 3ZT_e)$, where the second term describes the acceleration in the sheath, that depends on the ion charge. The ion stage distribution varies during an ELM cycle, when higher charged ions are swept out from the ETB and hit the limiter. An example for the temporal evolution of the W influx is given in the upper left graph of Fig.1,

which gives results for the modelling of a phase with 100 Hz ELM frequency of discharge #22895. The blue curve shows the influx change due to the increased losses of C, O, and W without considering the changes in the sputtering yield. For the red curve, only the temperature change at constant charge distribution is considered, while the black curve is calculated taking all effects into account. The ELM contributes 73% to the time integrated influx during one ELM cycle of 10 ms duration.

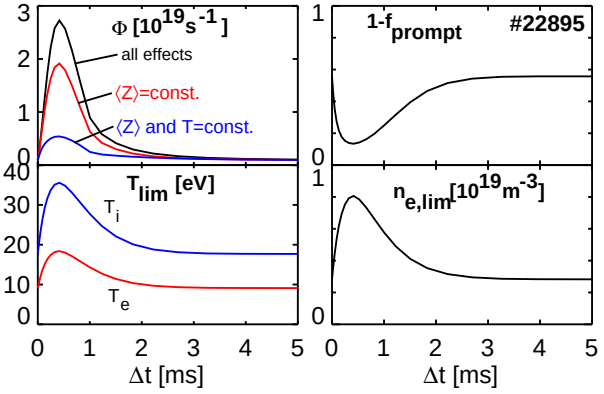

Fig.1: *Temporal evolution of the tungsten influx and the fraction of not promptly redeposited W during an ELM cycle. The used values for T_e, T_i and n_e at the limiters are shown in the lower graphs.*

From the energy of the sputtering impurity a mean neutral velocity for the sputtered W is calculated assuming a Thompson distribution. The ionisation length of W is in the range of the Larmor radius of the ionised tungsten and a fraction f_{prompt} of ionised W returns to the surface on the first travel along the Larmor radius. This prompt redeposition effect is included for the sputtering by each ion species. To this end, we use the result for a $\cos\theta$ angular velocity distribution in a homogeneous plasma, where $f_{prompt} = 1/(1 + (\Delta t_{ion}\omega_c)^2)$, and integrate it over the whole distribution of times Δt_{ion} to reach the ionisation radius. This simplified treatment yields nearly the same values for f_{prompt} as the correct integration over the angular distribution in a plasma with radial gradients and is justified considering the uncertainty about the angular distribution. In Fig.1, the upper right graph shows the part of the ionised tungsten that is not promptly redeposited, where the toroidal field was $B_t = 2.5$ T. During the ELM, the rise of n_e and T_e lead to shorter ionisation lengths and thus enhanced prompt redeposition. From the influx during on ELM cycle, 29% is not promptly redeposited.

The simultaneous treatment of light impurities and tungsten is also needed for the calculation of the collisional transport parameters in the ETB. For carbon and other light impurities, the transport in the ETB between ELMs has been found to be in accordance with neo-classical transport coefficients [4, 5]. Since it is characterised by a strong inwardly directed Pfirsch-Schlüter (PS) pinch, it is assumed that tungsten transport in the ETB is also dominated by PS transport leading to even higher pinch velocities due to the higher charge. The collisional transport of tungsten is dominated by collisions with low-Z impurities and it is necessary to include impurity-impurity collisions in the calculation of the PS transport coefficients of W. With increasing low-Z impurity concentration the diffusion coefficient D_{PS} increases. Furthermore, the low-Z impurities lead to a dilution of the deuterium ions. Thus, the n_D profile has a decreasing gradient with increasing low-Z concentration in the ETB and the PS inward pinch of tungsten decreases. The elements

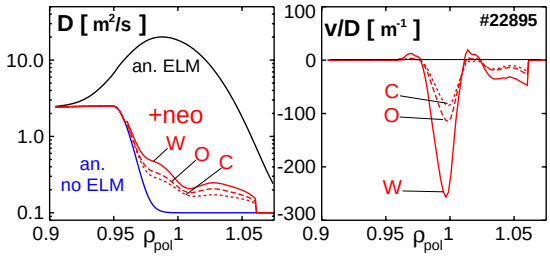

Fig.2: *Profiles of diffusion coefficient and drift parameter for the modelling of #22895.*

of the radial transport model are depicted in Fig.2, which is again for #22895. In the phase between ELMs, the anomalous diffusion coefficient (blue curve) was reduced in the ETB to a low value of 0.1 m^2/s. The collisional values from classical and PS transport are much larger with highest values for W. The red curves show the sum of both contributions for each element. The total value of the drift parameter v/D in this phase are shown in the right box, where W has the strongest inwardly directed drift. It is just calculated from the collisional pinch which depends on the impurity charge. The mean charge at poloidal flux label ρ_{pol}=0.99 is 5.6 for C, 7.4 for O and 16 for W. An ELM is induced by a sudden switch-on of a large diffusion coefficient in the edge (black curve), which decays linearly within 1 ms.

The resulting evolution of the total W density during an ELM cycle of #22895 is shown in Fig.3. The cycle has been repeated up to quasi-equilibrium, i.e. the density profile at the end and at the beginning of the cycle are equal. The density gradient around the separatrix is strongly degraded during the ELM and the increasing source from the limiter, which is at ρ_{pol}=1.063, leads to a density rise in the outer SOL. After the ELM, the source decreases and a strong density gradient forms in the ETB. The ratio of the tungsten density at ρ_{pol}=0.9 to the value at ρ_{pol}=1 is 22 at the end of the cycle and 7.2, when taking the temporal average during an ELM cycle. For a similar discharge #22901, which had 10 times less deuterium puff and an ELM frequency of about 50 Hz, the respective density ratios are 51 and 17.

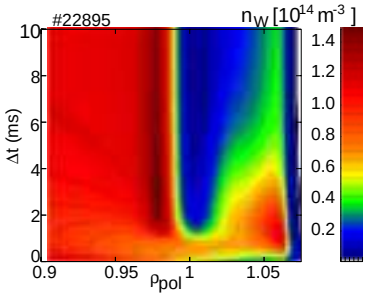

Fig.3: *Modelled evolution of the total W density during one ELM cycle.*

Modelling Procedure and Results

Three discharge phases with different deuterium puff levels Φ_D and ELM frequencies were modelled #22898: Φ_D=1.5×10^{22} s^{-1}, f_{ELM}≈200 Hz, #22895: Φ_D=10^{22} s^{-1}, f_{ELM}≈100 Hz, and #22901: Φ_D=10^{21} s^{-1}, f_{ELM}≈50 Hz. Average profiles of n_e, T_e and T_i were fitted for equal time delays to the ELM start using a 500 ms long discharge period. For each quantity a profile with time delays in the range 0-2 ms after the ELM and 4-2 ms before the ELM was fitted. A simplified time evolution of the profiles during an ELM cycle was generated using a temporal shape $f(\Delta t) = (\Delta t/\tau_c)\exp[-\Delta t/\tau_c]$ to switch on and off the ELM profile, where the characteristic time τ_c=0.4 ms was used. The carbon influx level was set ad hoc and complete recycling of the carbon loss to the wall was used. The influx level was chosen to get a fit of the measured C concentration at $\rho_{pol} = 0.95$ which was 0.9% for #22898, 1.2% for #22895, and 2.1% for #22901. The oxygen influx was set to 1/4 of the carbon influx. The T_i profiles from edge CXRS do not extend into the far SOL and the T_e profiles from Thompson scattering are too uncertain in the far SOL in order to decide whether the temperature at the limiter is 10 or 15 eV, which has a dramatic effect on the sputtering yield. Thus, the ELM and inter-ELM value of T_e and T_i at the limiters were prescribed in order to get the measured tungsten influx from the outboard limiters, which were shown to be the dominant source for the tungsten concentration in the confined plasma [1]. Here, $T_i = 2T_e$ was taken and the adjustments were done until the temporally averaged influx as well as the ELM contribution to the influx, which is about 70% for all ELM frequencies, was fitted. The used inter-ELM and ELM values for T_e at the limiter were

8.4 eV/12 eV for #22898, 10 eV/20 eV for #22895, and 12 eV/35 eV for #22901. Only 1/3 of the low-Z impurity losses were considered for the W production at the outboard limiters. This choice reflects the difference in the poloidal profile of the impurity penetration for W and low-Z impurities, where the latter are assumed to pentrate equally well from low- and high-field side plasma facing components.

The transport model for each input parameter set was solved until temporal equilibrium was reached. This was done for an artificial scan of the ELM frequency with f_{ELM}=0, 50, 100, and 200 Hz using all three settings for the background profiles, limiter temperatures and low-Z fluxes. Fig.4 shows a number of key quantities for these scans. Black curves are for the settings of #22898, blue for #22895, and red for #22901. The black circles surround the points, for which the limiter temperatures, ELM sizes, and influx values were adjusted to the measurement. The upper left box shows the strong decrease of the W density peaking with increasing ELM frequency, which can reach values on the order of 100 for the artificial zero ELM case. The plasma with the lowest puff level has the highest peaking factors. The particle confinement time τ_p of W (lower left box) is calculated with the total number of W ions in the confined region N_W and the total source Φ. It decreases strongly with the ELM frequency. The higher parallel losses for the low puff plasma with higher SOL temperatures leads to slightly lower τ_p than for the high puff case. In the upper right box, the increase of the erosion source with f_{ELM} is due to the linear picture without taking the change of the ELM size and the lower inter-ELM temperatures into account. The encircled points reflect the measured behaviour. Nevertheless, the rise of the source is not strong enough to beat the change in τ_p and c_W at ρ_{pol}=0.8 decreases on each of the *linear* curves, as shown in the lower right box. Going along the encircled points the values are 3.5x10^{-5}, 1.6x10^{-5}, and 8.7x10^{-6} from low to high ELM frequency. The drop from 50 to 100 Hz is due to the decay in τ_p and from 100 to 200 Hz due to the drop in Φ. The calculated c_w values are actually within 10% of the measured values 3.6x10^{-5}, 1.8x10^{-5}, and 8.4x10^{-6}. Even though this is an encouraging result, we consider the model only to be a consistent description based on many ad hoc assumptions, which need further detailed experimental investigations. However, it seems, that we captured the dominant mechanisms to understand the tungsten particle confinement.

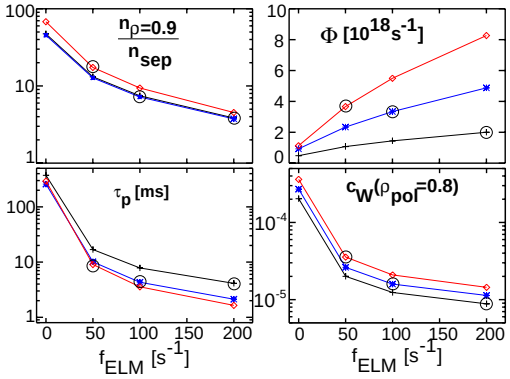

Fig.4: *Calculated edge density ratio, source rate, particle confinement time and W concentration for a scan of the ELM frequency. All quantites are temporal averages of one ELM cycle.*

References

[1] R. Dux, et al., J. Nucl. Mater. **390-391**, 858 (2009).
[2] R. Dux, Rep. IPP 10/30, Max-Planck-Institut für Plasmaphysik, Garching (2006).
[3] W. Eckstein, et al., Rep. IPP 9/82, Max-Planck Institut für Plasmaphysik, Garching (1993).
[4] T. Pütterich, et al.,*Proc. of the 35rd EPS Conf.*, vol. 32F, P–2.083, Geneva (2008).
[5] T. Pütterich, et al.,*this conference* (2009).